arXiv:hep-ph/9810284v1 8 Oct 1998

Valence quark annihilation effect on charmed meson production in πN collisions

Tsutomu Tashiro[1], Hujio Noda[2], Kisei Kinoshita[3] and Shin-ichi Nakariki[1]

[1]Department Simulation Physics, Okayama University of Science, Ridai-cho, Okayama 700-0005, Japan
[2]Department of Mathematical Science, Faculty of Science, Ibaraki University, Bunkyou, Mito 310-0056, Japan
[3]Physics Department, Faculty of Education, Kagoshima University, Korimoto, Kagoshima 890-0065, Japan

Abstract

We discuss the hadroproduction of charmed mesons in the framework of the constituent cascade model taking into account the valence quark annihilation. It is shown that the small valence quark annihilation process dominates the leading particle production at large Feynman x and explains the recent experimental data on the asymmetry between D^0 and $\bar{D}^0$ at 350 GeV/c.

PACS
13.75.Gx(Pion-baryon interactions)
13.87.Fh(Fragmentation into hadrons)
14.40.Lb(Charmed mesons)

[1] email: tashiro@sp.ous.ac.jp, nakariki@sp.ous.ac.jp, Fax: +81 86 256 8006
[2] email: noda@mito.ipc.ibaraki.ac.jp, Fax: +81 29 228 8407
[3] email: kisei@rikei.edu.kagoshima-u.ac.jp, Fax: +81 99 285 7735

1 Introduction

Recently experiments at CERN [1] measured the neutral D mesons in π^- nucleus collisions and observed much smaller values of the leading/non-leading asymmetry than those of charged D mesons i.e. less than 0.2 and even a negative value around $x = 0.8$. The experimental data on the asymmetry of charged D mesons increases from zero to nearly one with Feynman variable x in the π^- fragmentation region [1, 2, 3, 4, 5]. The leading particle contains the same type of quark as one of the valence quarks in the incident hadron, while the non-leading one does not contain the projectile valence quarks. For example, the asymmetry of $D^0(c\bar{u})/\bar{D}^0(u\bar{c})$ in $\pi^-(d\bar{u})$ interaction with nucleon is defined as

$$A_{\pi^- N}(D^0, \bar{D}^0) = \frac{\sigma(D^0) - \sigma(\bar{D}^0)}{\sigma(D^0) + \sigma(\bar{D}^0)}. \tag{1}$$

In the perturbative QCD at leading order, the factorization theorem predicts that c and $\bar{c}$ quarks are produced with the same distributions and then fragment independently. In this case the asymmetry $A_{\pi^- N}(D^-, D^+)$ is equal to zero [6]. Even in the case of next to leading order, the predicted asymmetry is much smaller than the data [7]. The asymmetry $A_{\pi^- N}(D^-, D^+)$ has been investigated and explained by means of many approaches: string fragmentation [8], intrinsic charm contributions [9, 10, 11, 12, 13, 14], recombination process [15, 16, 17], recombination using valon concept [18, 19] and so on. We have proposed the constituent quark-diquark cascade model and explained the leading/non-leading asymmetry of charged D mesons $A_{\pi^- N}(D^-, D^+)$ successfully [20]. The model, however, gives rather large values of $A_{\pi^- N}(D^0, \bar{D}^0)$ at $0.5 \lesssim x$ as expected from the leading particle effect but deviating from the experimental data. Although several models have been applied more or less satisfactorily to $A_{\pi^- p}(D^0, \bar{D}^0)$ at $x \lesssim 0.6$ [14, 17], the asymmetry problem about the charmed hadron productions is an open question.

In the present paper we investigate the leading/non-leading D-meson asymmetry in the framework of the constituent quark-diquark cascade model by taking into account the valence quark annihilation.

2 Model description

We consider an inclusive reaction $A + B \to C + X$ in the centre of mass system of A and B. The light-like variables of A and B are defined as follows:

$$x^A_{0\pm} = \frac{E^A \pm p_{cm}}{\sqrt{s_0}}, \quad x^B_{0\pm} = \frac{E^B \mp p_{cm}}{\sqrt{s_0}}, \tag{2}$$

where $\sqrt{s_0}$ is the centre of mass energy of the incident hadrons A and B. We briefly review our model and then introduce the valence quark annihilation mechanism into the model.

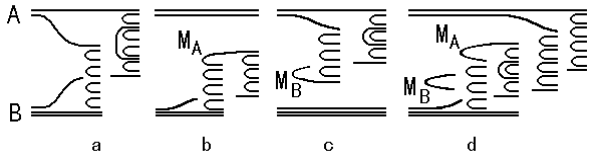

Figure 1: The interaction mechanism in AB collision: **a** Non-diffractive dissociation type, **b, c** Single-diffractive and **d** double diffractive dissociation type mechanisms.

When the collision between A and B occurs, the incident hadrons break up into two constituents with a probability $(1-P_{gl})$; otherwise they emit wee gluons with P_{gl} followed by a quark-antiquark pair creation. We assume four interaction types: a) non-diffractive dissociation, b) and c) single-diffractive dissociations of B and A, and d) double-diffractive dissociation types as shown in Fig. 1. The probabilities of these types to occur are $(1-P_{gl})^2, P_{gl}(1-P_{gl}), P_{gl}(1-P_{gl})$ and P_{gl}^2, respectively. Here we denote the quark-antiquark pair emitted from A (B) via the wee gluons as M_A (M_B). The probabilities of M_A (M_B) to be $u\bar{u}, d\bar{d}, s\bar{s}$ and $c\bar{c}$ are denoted as $P_{u\bar{u}}$, $P_{d\bar{d}}$, $P_{s\bar{s}}$ and $P_{c\bar{c}}$, respectively.

The momentum fraction of M_A is fixed by the distribution function

$$H_{M_A/A}(z) = z^{\beta_{gl}-1}(1-z)^{\beta_{ld}-1}/B(\beta_{gl},\beta_{ld}), \tag{3}$$

and the uniform distribution R in the interval from zero to one as,

$$x_+^{M_A} = x_{0+}^A z, \quad x_-^{M_A} = x_{0-}^A R. \tag{4}$$

Then the incident particles A and B have the following momentum fractions:

$$x_+^A = x_{0+}^A(1-z), \quad x_-^A = m_A^2/(x_+^A\ s_0),$$

$$x_-^B = x_{0-}^B - (x_-^A - x_{0-}^A(1-R)), \quad x_+^B = x_{0+}^B, \tag{5}$$

where the mass shell condition is considered and transverse momenta are neglected. The momentum fraction of M_B is treated similarly, exchanging the role of A and B.
In the centre of mass system of incidents $A(M_A)$ and $B(M_B)$, we define the light-like fractions of these hadrons and fix the light-like fractions of the projectile constituents. The distribution functions of the constituents in the projectile A composed of a and a' are described as

$$H_{a/A}(z) = H_{a'/A}(1-z) = \frac{z^{\beta_a-1}(1-z)^{\beta_{a'}-1}}{B(\beta_a,\beta_{a'})}. \tag{6}$$

Then the light-like fractions of a and a' are $x_+^a = x_{0+}^A z$,
$x_-^a = x_{0-}^A R$, $x_+^{a'} = x_{0+}^A - x_+^a$ and $x_-^{a'} = x_{0-}^A - x_-^a$, respectively. The distribution functions of the constituents in M_A, B and M_B are similarly defined.

In our model hadrons are produced on the chain between a valence quark(anti-quark) from $A(M_A)$ and the valence diquark(quark) from $B(M_B)$ via the cascade processes

$$\begin{aligned} q &\rightarrow M(q\bar{q}') + q', \\ &\quad B(q[q'q'']) + \overline{[q'q'']}, B(q\{q'q''\}) + \overline{\{q'q''\}}, \\ \overline{[q'q'']} &\rightarrow \overline{B}(\bar{q}\overline{[q'q'']}) + q, \\ &\quad M(q\bar{q}') + \overline{[qq'']}, M(q\bar{q}') + \overline{\{qq''\}}, \\ \overline{\{q'q''\}} &\rightarrow \overline{B}(\bar{q}\overline{\{q'q''\}}) + q, \\ &\quad M(q\bar{q}') + \overline{[qq'']}, M(q\bar{q}') + \overline{\{qq''\}}, \end{aligned} \tag{7}$$

where [ ] and {} denote the flavour antisymmetric and symmetric diquarks, respectively [21]. Meson production probabilities from $q, \overline{[q'q'']}$ and $\overline{\{q'q''\}}$ are $1-\epsilon, \eta_{[\,]}$ and $\eta_{\{\}}$, respectively.

We redefine the light-like fractions of the incident constituents in the rest frame of the cascade chain. The momentum sharing of the cascade process $q + \bar{q}' \rightarrow M(q\bar{q}'') + q'' + \bar{q}'$ from a q with $x_{\pm}^{q}$ and $\bar{q}'$ with $x_{\pm}^{\bar{q}'}$ takes place as follows [22, 23]: First, using the emission function

$$F_{q''q}(z) = z^{\gamma\beta_q - 1}(1-z)^{\beta_q + \beta_{q''} - 1}/B(\gamma\beta_q, \beta_q + \beta_{q''}), \tag{8}$$

we fix the lightlike fractions of q'' and M as $x_{+}^{q''} = x_{+}^{q} z$ and $x_{+}^{M} = x_{+}^{q} - x_{+}^{q''}$, respectively and put $x_{-}^{q''} = x_{-}^{q}$. Second, the transverse momentum of M is determined from the probability function

$$G(\boldsymbol{p}_T^2) = \frac{\sqrt{m}}{C} \exp(-\frac{C}{\sqrt{m}}\boldsymbol{p}_T^2) \tag{9}$$

in p_T^2 space. Then, from the onshell condition, x_{-}^{M} is fixed as $x_{-}^{M} = (m_M^2 + {\boldsymbol{p}_T}^2)/x_{+}^{M} s'$, where $\sqrt{s'}$ is the subenergy of the cascade chain. The transverse momentum of q'' is $\boldsymbol{p}_T^{q''} = \boldsymbol{p}_T^{q} - \boldsymbol{p}_T$. The lightlike fraction of $\bar{q}'$ is decreased to $\tilde{x}_{-}^{\bar{q}'} = x_{-}^{\bar{q}'} - x_{-}^{M}$. If the energy of $\bar{q}'$ is enough to create another hadron, the cascade such as $q'' + \bar{q}' \rightarrow q'' + \bar{q}''' + M(q'''\bar{q}')$ takes place in the opposite side. Finally recombined hadrons are put on-shell by a two body decay process as explained in [20].

The dynamical parameters β's in (6) and (8), which determine the momentum sharings of the constituents, are related to the intercepts of the Regge intercepts as $\beta_u = \beta_d = 1 - \alpha_{\rho-\omega}(0)$, $\beta_s = 1 - \alpha_{\phi}(0), \beta_c = 1 - \alpha_{J/\psi}(0)$ [24, 25]. From previous analyses [21, 22], we determine the values for diquarks as $\beta_{[ij]} = \gamma_{[\,]}(\beta_i + \beta_j)$, $\beta_{\{ij\}} = \gamma_{\{\}}(\beta_i + \beta_j)$. We consider lower lying hadrons: pseudoscalar(PS), vector (V), tensor(T) mesons, octet(O) and decuplet(D) baryons composed of u, d, and s flavours and the correspondings with charm flavour. We assume the production probabilities for them to be P_{PS}, P_V, P_T $(= 1 - P_{PS} - P_V), P_O$ and P_D $(= 1 - P_O)$, respectively. Octet and decuplet baryons are described as

$$|8> = \cos\theta |q[q'q''] > + \sin\theta |q\{q'q''\} >, \tag{10}$$

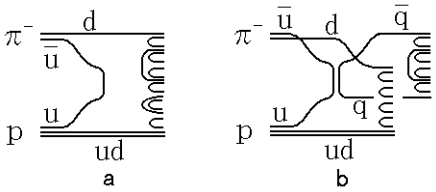

Figure 2: The valence quark annihilation processes **a** soft annihilation and **b** semi-hard annihilation processes in $\pi^- p$ collision.

$$|10>=|q\{q'q''\}> . \tag{11}$$

Directly produced resonances decay into stable particles. Details of our model are explained in [20, 21, 22].

We modify our model to include valence quark annihilation in the non-diffractive dissociation type interaction. Let us consider the case of $\pi^- p$ collision. We take account of the annihilation of the valence $\bar{u}$ from π^- and valence u from proton target in a slightly different way from the one pointed out in [15, 17]. There are annihilation processes such as shown in Fig.2. The annihilation process in Fig.2a is considered soft process and its contribution is related to the magnitude of $\sigma_{inel}^{\pi^-} - \sigma_{inel}^{\pi^+}$ by unitarity. This process, however, may be negligible for the charm-pair production. Here we only take into account the annihilation process in Fig.2b and assume that the process

$$\bar{u}u \to \bar{q}q \tag{12}$$

occurs with the probability $P_{anni}(1-P_{g\ell})^2$ and the non-diffractive type occurs with the probability $(1-P_{anni})(1-P_{g\ell})^2$. Branching ratios of $\bar{u}u \to \bar{u}u, \bar{d}d, \bar{s}s$, and $\bar{c}c$ are chosen to be equal to each other for the channels allowed energetically.

This process is considered as a semi-hard scattering process and produced q and $\bar{q}$ are supposed to be non-free. It seems natural to assume that $\bar{q}$ has tendency to be produced in the forward direction of the $\bar{u}$ in the centre of mass system of $\bar{u}$ and u, due to the confinement force between the valence d quark and the produced $\bar{q}$ quark. Here we choose the distributions for $z = \cos\phi$ as

$$D(z) = \frac{3}{8}(1+z)^2 \tag{13}$$

in the region $-1 < z < 1$, where ϕ is the angle between the directions of $\bar{u}$ and $\bar{q}$ in the centre of mass system of $\bar{u}$ and u. After this annihilation mechanism, the non-diffractive type production of hadrons occurs as shown in Fig. 2b.

3 Comparison with the data

In this section, we give the results of our model for the inclusive hadron productions in $\pi^- N$ collisions. The value of the dynamical parameter β_c is changed from the value

$\beta_c = 8.0$ used in [20] to $\beta_c = 4.0$. This is in accord with the argument that the slopes of Regge trajectories of charmed mesons are smaller than those of light mesons as discussed in [26]. The parameter of p_T^2 distribution $C = 1.2$ and the probability $P_{c\bar{c}} = 0.00016 (P_{s\bar{s}} = 0.09984)$ in [20] are changed into $C = 1.0$ and $P_{c\bar{c}} = 0.00025 (P_{s\bar{s}} = 0.09975)$. Furthermore the meson production probabilities are assumed as $P_{PS} = 0.4, P_V = 0.4$ and $P_T = 0.2$ for light mesons and $P_{PS} = 1/9, P_V = 1/3$ and $P_T = 5/9$ for charmed mesons. We put the parameter P_{anni} so as to reproduce the asymmetry $A_{\pi^- N}(D^0, \bar{D}^0)$. We choose the value $P_{anni} = 0.0005$. This value scarcely changes the features of the spectra of light hadrons with u, d and s. For other parameters, we use the same values used in the previous analysis [20].

In Fig.3 we show the results of D^* productions and compare the two cases: case(1) $3(1+z)^2/8$ distribution for $\cos\alpha$ and case(2) without annihilation ($P_{anni} = 0$:the same as in [20] except for the values of $\beta_c = 4.0, C = 1.0, P_{c\bar{c}} = 0.00025$, and $P_{PS} = 1/9, P_V = 1/3$ and $P_T = 5/9$ for charmed meson productions). The annihilation effect of Fig.2b is seen in $\bar{D}^{*0}(u\bar{c})$ and $D^{*-}(d\bar{c})$. Our model gives a satisfactory description of x dependence for production of D^{*+} or D^{*-} in $\pi^- N$ collision. The result for production of D^{*0} or $\bar{D}^{*0}$ at $x \approx 0.1$ is small as compared with experimental data [27].

The annihilation effect on meson productions in $\pi^- p$ is twice as much as in $\pi^- n$ collision. The annihilation mechanism have a considerable effect on the non-leading particle $\bar{D}^{*0}(u\bar{c})$. However, the shape of the leading particle $D^{*-}(d\bar{c})$ is affected little by the annihilation mechanism. Therefore our model gives larger differences between $A_{\pi^- p}(D^{*0}, \bar{D}^{*0})$ and $A_{\pi^- n}$ $(D^{*0}, \bar{D}^{*0})$ than those between $A_{\pi^- p}(D^{*-}, D^{*+})$ and $A_{\pi^- n}(D^{*-}, D^{*+})$. Fig.4a shows the results in case(1) for $A_{\pi^- p}(D^{*0}, \bar{D}^{*0})$, $A_{\pi^- n}(D^{*0}, \bar{D}^{*0})$ and $A_{\pi^- N}(D^{*0}, \bar{D}^{*0})$. Hereafter we show the average results of π^- beam on proton and neutron targets. Fig.4b shows the results of $A_{\pi^- N}(D^{*0}, \bar{D}^{*0})$ and $A_{\pi^- N}(D^{*-}, D^{*+})$ in case(1) and case(2).

Smaller values of $A_{\pi^- N}(D^{*-}, D^{*+})$ as compared with $A_{\pi^- N}(D^{*0}, \bar{D}^{*0})$ at $x \approx 0.5$ are due to the difference between the hadron productions on quark-diquark and antiquark-quark chains in non-diffractive dissociation type mechanism (Fig.1a) [20]. The leading particle $D^{*-}(d\bar{c})$ is produced on the chain between the valence d quark in the beam and the valence diquark in the target. The proton target has a tendency to break into an energetic valence diquark and a wee valence quark. Then the D^{*-} meson produced in the first cascade step is energetic. However, in the case in which a baryon is produced from the valence diquark in the first cascade step, the momentum of the valence d quark is decreased. Furthermore the total momentum is shifted to the diquark side. Then the leading spectrum of D^{*-} on the quark-diquark chain tends to have a small momentum and the asymmetry is reduced in $0.3 \lesssim x \lesssim 0.7$.

On the other hand, the leading particle $D^{*0}(c\bar{u})$ is produced on the chain between the valence $\bar{u}$ quark in the π^- beam and the valence quark in the target. The momentum reduction of the $\bar{u}$ quark is small even in a case a meson is produced in the first cascade step from the valence quark in the target fragmentation. Therefore the asymmetry $A_{\pi^- N}(D^{*0}, \bar{D}^{*0})$ is not so suppressed as compared with $A_{\pi^- N}(D^{*-}, D^{*+})$ in $0.3 \lesssim x \lesssim 0.7$. In case(1), the annihilation effect compensates the quark-diquark effect and the asymmetry $A_{\pi^- N}(D^{*0}, \bar{D}^{*0})$ becomes negative at large x.

In Fig. 5, we show the result of x dependence of D mesons in $\pi^- N$ collisions for case(1) and case(2). The annihilation effect is also seen in $\bar{D}^0$ and a little in D^- spectra as in D^* spectra. In Fig. 6, we show the result of p_T^2 dependence of D mesons in $\pi^- N$ collisions for case(1) and case(2). Our calculation shows smaller values of D^0 than those of $\bar{D}^0$ at large p_T^2 deviating from the data. The newly introduced annihilation process explains the large p_T^2 charmed meson productions in part. Our model is in good agreement with the data except for D^0, $\bar{D}^0$ at large p_T^2. In Fig. 7 the results of x dependence of $A_{\pi^- N}(D^-, D^+)$ and $A_{\pi^- N}(D^0, \bar{D}^0)$ are compared with the experimental data at 350 GeV/c [1]. The agreement of x dependence with the experimental data is satisfactory. The negative value of $A_{\pi^- N}(D^0, \bar{D}^0)$ at large x is well explained by introducing a small amount of the valence quark annihilation process to the model. Fig.8 presents the results of p_T^2 dependence of $A_{\pi^- N}(D^-, D^+)$ and $A_{\pi^- N}(D^0, \bar{D}^0)$. The p_T^2 dependence of $A_{\pi^- N}(D^0, \bar{D}^0)$ disagrees with the data in sign as seen in Fig.6b. The discrepancy increases with the annihilation effect. The results of the x and p_T^2 dependences of $A_{\pi^- N}(D^-, D^+)$ and $A_{\pi^- N}(D^0, \bar{D}^0)$ at 500 GeV/c are compared with the experimental data [4] in Fig.9. The agreement with the data is fairly good except for the negative value of the data at $x \approx -0.15$. There is a valence d quark in the incident nucleon and our model predicts a positive value of $A_{\pi^- N}(D^-, D^+)$ for $x < 0$ as seen in Fig.9. However, in the case of proton target with $\cos\theta = 1$ in (10), there is no valence d quark and the model gives a small value of $A_{\pi^- N}(D^-, D^+)$ in the target fragmentation region.

The results of the x and p_T^2 dependence for production of $D_S^-(s\bar{c})$ or $D_S^+(c\bar{s})$ are compared with the experimental data [1] in Fig.10. The features of the spectra are in good agreement with the data except for the small discrepancy in normalization. Fig.11 shows the calculated results of asymmetries $A_{\pi^- N}(D_S^-, D_S^+)$ with respect to x and p_T^2. The values are small because both $D_S^\pm$ mesons are non-leading particles. But in case(1) $A_{\pi^- N}(D_S^-, D_S^+)$ increases with x at large x due to the valence quark annihilation.

4 Discussions

The large leading/non-leading asymmetry $A_{\pi^- N}(D^-, D^+)$ is naturally explained by our constituent quark cascade model as in the case of light hadron productions. In [20], we noticed that the cascade chain properties are different between the antiquark-quark and the quark-diquark chains. The leading particle $D^-(d\bar{c})$ produced in the quark-diquark chain in $\pi^- p$ collision is less energetic when a baryon is produced in the target fragmentation in the first cascade process as compared with $D^+(c\bar{d})$ produced in the quark-antiquark chain in $\pi^+ p$ collision. We have different leading particle effects between π^+ and π^- beams i.e. $A_{\pi^+ N}(D^+, D^-) > A_{\pi^- N}(D^-, D^+)$ around $x \sim 0.6$ [20]. Although the difference between the asymmetries $A_{\pi^- N}(D^0, \bar{D}^0)$ and $A_{\pi^- N}(D^-, D^+)$ disappears due to the decay effect and the valence quark annihilation effect,this quark-diquark chain effect is seen in the difference between the asymmetries $A_{\pi^-}(D^{*0}, \bar{D}^{*0})$ and $A_{\pi^- N}(D^{*-}, D^{*+})$
around $x \sim 0.5$ as shown in Fig.4b.

The small valence quark annihilation process (12) explains the negative value of

$A_{\pi^- N}(D^0, \bar{D}^0)$ at large x observed in the recent experiment [1]. This process is considered as semi-hard interaction. All channels occur with equal probability and the produced constituents tend to have the forward direction of the incident valence constituents. This is a part of the hadron production process at large p_T^2. Our model can explain the spectra up to the region $p_T^2 \lesssim 10$ (GeV/c)^2. As noticed in the previous section, the results of calculated behaviours of the p_T^2 dependence of $A_{\pi^- N}(D^0, \bar{D}^0)$ disagree with the experimental data. This implies that there may be considerable contribution from soft interactions which maintain the leading particle effect even at large p_T^2 region. The negative values of experimental data on $A_{\pi^- N}(D^0, \bar{D}^0)$ at $p_T^2 \lesssim 3$ (GeV/c)^2 suggests that the $\bar{q}$ quark in the annihilation process (12) is produced in the very small cone around the direction of incident $\bar{u}$ as compared with (13). It is interesting to investigate the leading/nonleading asymmetry in KN collisions, since in K^+N collision, there is no annihilation process. These points will be discussed elsewhere.

References

[1] M. Adamovich et al., (WA92): Nucl. Phys. **B495**, 3(1997)

[2] M. Adamovich et al., (WA82): Phys. Lett. **B305**, 402(1993)

[3] G. A. Alves et al., (E769): Phys. Rev. Lett. **72**, 812(1994)

[4] E. M. Aitala et al., (E791): Phys. Lett. **B371**, 157(1996)

[5] G. A. Alves et al., (E769): Phys. Rev. Lett. **77**, 2388(1996)

[6] J. Qiu and G. Sterman: Nucl. Phys. **B353**, 105, 137(1991)

[7] P. Nason, S. Dawson, K. Ellis: Nucl. Phys. **B327**, 3(1989)

[8] H. U. Bengtsson, T. Sjöstrand: Comput. Phys. Commun. **46**, 43(1987); E. Norrbin, T. Sjöstrand: hep-ph/9809266

[9] R. Vogt, S. J. Brodsky: Nucl. Phys. **B438**, 261(1995); R. Vogt: Z. Phys. **C71**, 475(1996)

[10] G. Anzivino et al.: Nuovo Cim. **107A**, 955(1994)

[11] N. Armesto, C. Pajares, Yu. M. Shabelski: Preprint of Universidade de Santiago de Compostela, hep-ph/9506212, 1995

[12] O. I. Piskounova: Nucl. Phys. Proc. Suppl. **50**, 179(1996)

[13] G. H. Arakelyan, P. E. Volkovitsky: Z. Phys. **A353**, 87(1995)

[14] G. H. Arakelyan: Preprint of JINR, hep-ph/9711276, Nov. 1997

[15] V. A. Bednyakov: Mod. Phys. Lett. **A10**, 61(1995)

[16] J. C. Anjos et al.: Phys. Rev. **D56**, 394(1997); hep-ph/9702256

[17] E. Cuautle, G. Herrera, J. Magnin: Eur. Phys. J. **C2**, 473(1998)

[18] R. C. Hwa: Phys. Rev. **D51**, 85(1995)

[19] K. P. Das, R. C. Hwa: Phys. Lett. **68B**, 459(1977)

[20] T. Tashiro, H. Noda, S. Nakariki, K. Ishii, K. Kinoshita: Eur. Phys. J. **C2**, 733(1998)

[21] K. Kinoshita, H. Noda, T. Tashiro: Prog. Theor. Phys. **68**, 1699, 2086(1982); T. Tashiro, H. Noda, K. Kinoshita, C. Iso: Z. Phys. **C35**, 21(1987)

[22] K. Kinoshita, H. Noda, T. Tashiro, J. Nagao: *Int. Symp. on High Energy Nuclear Collisions and Quark Gluon Plasma*, Kyoto 1991, edited by M. Biyajima, H. Enyo, T. Kunihiro, O. Miyamura(World Science, Singapore 1993)245

[23] K. Kinoshita, A. Minaka: Prog. Theor. Phys. **81**, 183(1989)

[24] H. Minakata: Phys. Rev. **D20**, 1656(1979)

[25] G. Cohen-Tannoudji, A.El Hassouni, J. Kalinowski, R. Peschanski: Phys. Rev. **D19**, 3397(1979)

[26] L. Burakovsky, T. Goldman: LA-UR-98-492(hep-ph/9802247)

[27] M. Aguilar-Benitez et al.: Phys. Lett. **169B**, 106(1986)

Figure 3: Comparison of the model with the experimental data on the x-dependences for productions of **a** D^{*+} or D^{*-} and **b** D^{*0} or $\bar{D}^{*0}$ mesons at $P_L = 360$ GeV/c [27]. The theoretical lines were calculated for $P_L = 350$ GeV/c, full line for case(1) with the valence quark annihilation and dotted for case(2) without the valence quark annihilation.

Figure 4: **a** The x-dependences of the asymmetries $A_{\pi^- p}(D^{*0}, \bar{D}^{*0}), A_{\pi^- n}(D^{*0}, \bar{D}^{*0})$ and $A_{\pi^- N}(D^{*0}, \bar{D}^{*0})$. **b** The comparison of x-dependence of the asymmetries $A_{\pi^- N}(D^{*0}, \bar{D}^{*0})$ and $A_{\pi^- N}(D^{*-}, \bar{D}^{*+})$ between in the case(1) and case(2).

Figure 5: The x-dependences of **a** $D^{\pm}$ and **b** D^0 and $\bar{D}^0$ mesons at $P_L = 350$ GeV/c. The full lines were calculated for case(1) with the valence quark annihilation and dotted for case(2) without the valence quark annihilation. The experimental data are taken from [1].

Figure 6: Same as in Fig.5 for p_T^2-dependence in range $0 \leq x \leq 1$.

Figure 7: The x-dependences of asymmetries **a** $A_{\pi^- N}(D^-, D^+)$ and **b** $A_{\pi^- N}(D^0, \bar{D}^0)$ at $p_L = 350$ GeV/c. The full lines show the results in case(1) and dotted lines in case(2). The experimental data are taken from [1].

Figure 8: Same as in Fig.7 for p_T^2-dependences in range $0 \leq x \leq 1$.

Figure 9: The asymmetry $A_{\pi^- N}(D^-, D^+)$ at $p_L = 500$ GeV/c **a** as a function of x, **b** as a function of p_T^2 for range of $-0.2 \leq x \leq 0.8$ and $0.4 \leq x \leq 0.8$. The experimental data are taken from [4].

Figure 10: Differential cross sections with respect to **a** x and **b** p_T^2 for production of D_S^+ or D_S^- at $P_L = 350$ GeV/c. The full line denotes the results for case(1) and dotted for case(2). The experimental data are taken from [1].

Figure 11: Asymmetries $A_{\pi^- N}(D_S^-, D_S^+)$ with respect to **a** x and **b** p_T^2 for at $P_L = 350$ GeV/c. The full line denotes the results for case(1) and dotted for case(2).

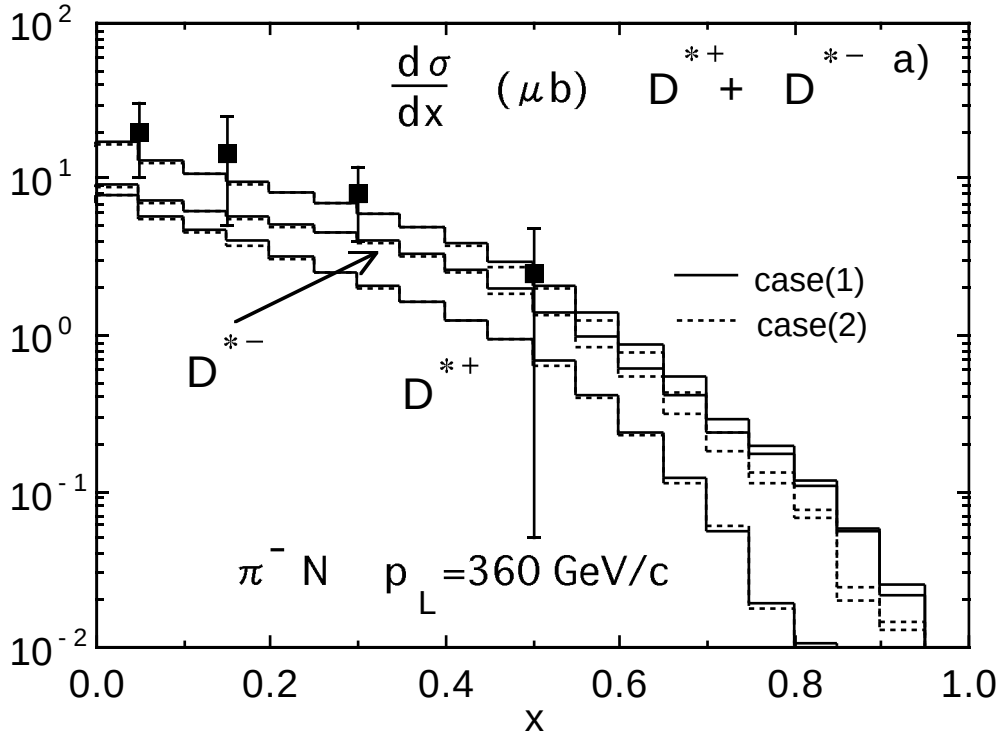
10^2
10^1
10^0
10^{-1}
10^{-2}
$\frac{d\sigma}{dx}$ (μb) $D^{*+} + D^{*-}$ a)
case(1)
case(2)
D^{*-}
D^{*+}
π^- N p_L=360 GeV/c
0.0
0.2
0.4
0.6
0.8
1.0
x

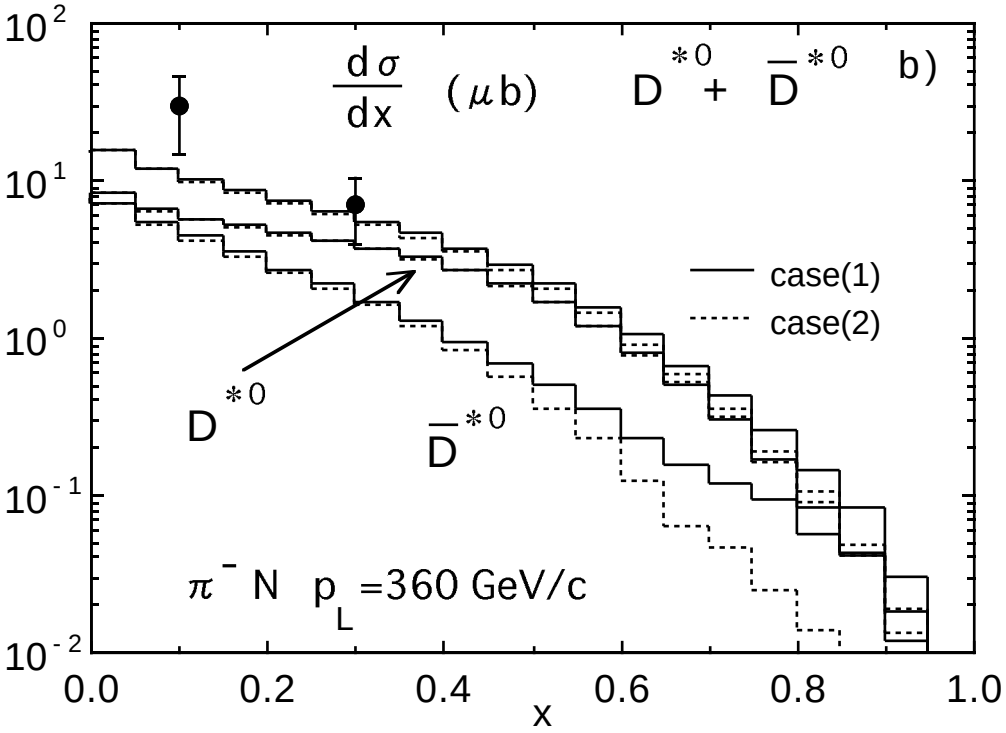
10^2
10^1
10^0
10^{-1}
10^{-2}
$\frac{d\sigma}{dx}$ (μb) $D^{*0} + \overline{D}^{*0}$ b)
case(1)
case(2)
D^{*0}
$\overline{D}^{*0}$
π^- N p_L=360 GeV/c
0.0
0.2
0.4
0.6
0.8
1.0
x

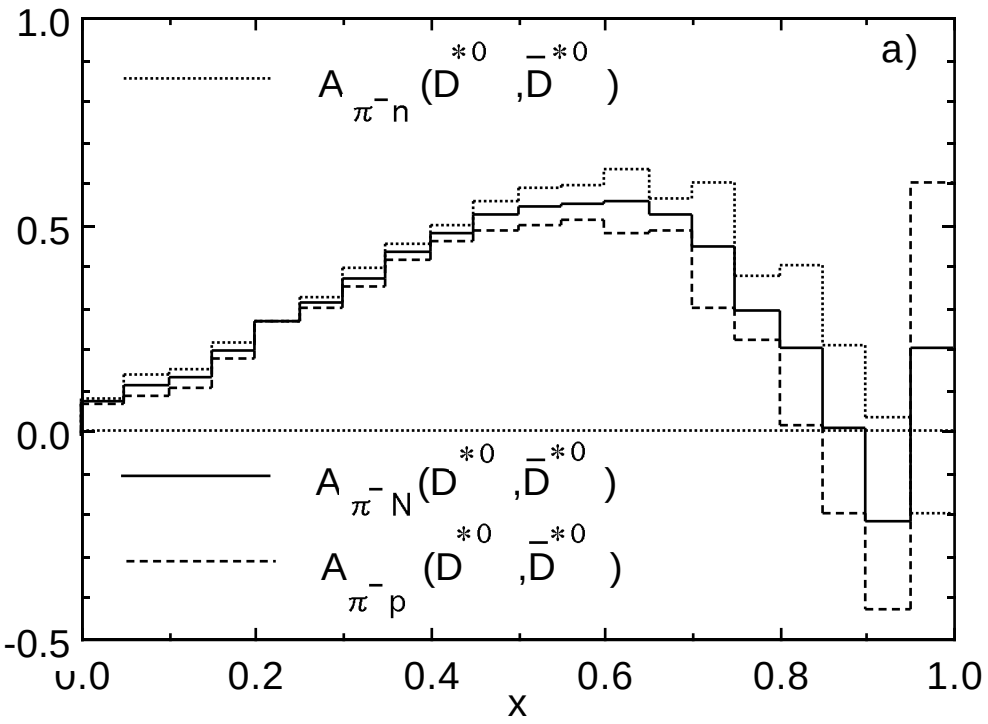
1.0
0.5
0.0
-0.5
0.0
0.2
0.4
0.6
0.8
1.0
x
a)
$A_{\pi^- n}(D^{*0}, \bar{D}^{*0})$
$A_{\pi^- N}(D^{*0}, \bar{D}^{*0})$
$A_{\pi^- p}(D^{*0}, \bar{D}^{*0})$

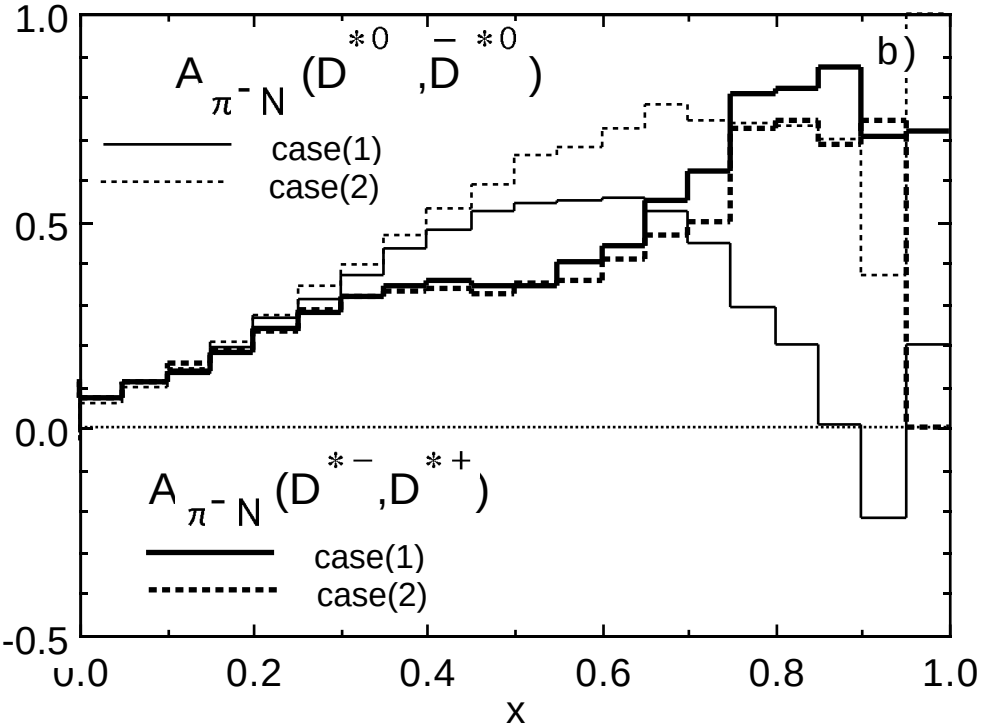
1.0
0.5
0.0
-0.5
0.0
0.2
0.4
0.6
0.8
1.0
x
b)
$A_{\pi^- N}(D^{*0}, \bar{D}^{*0})$
case(1)
case(2)
$A_{\pi^- N}(D^{*-}, D^{*+})$
case(1)
case(2)

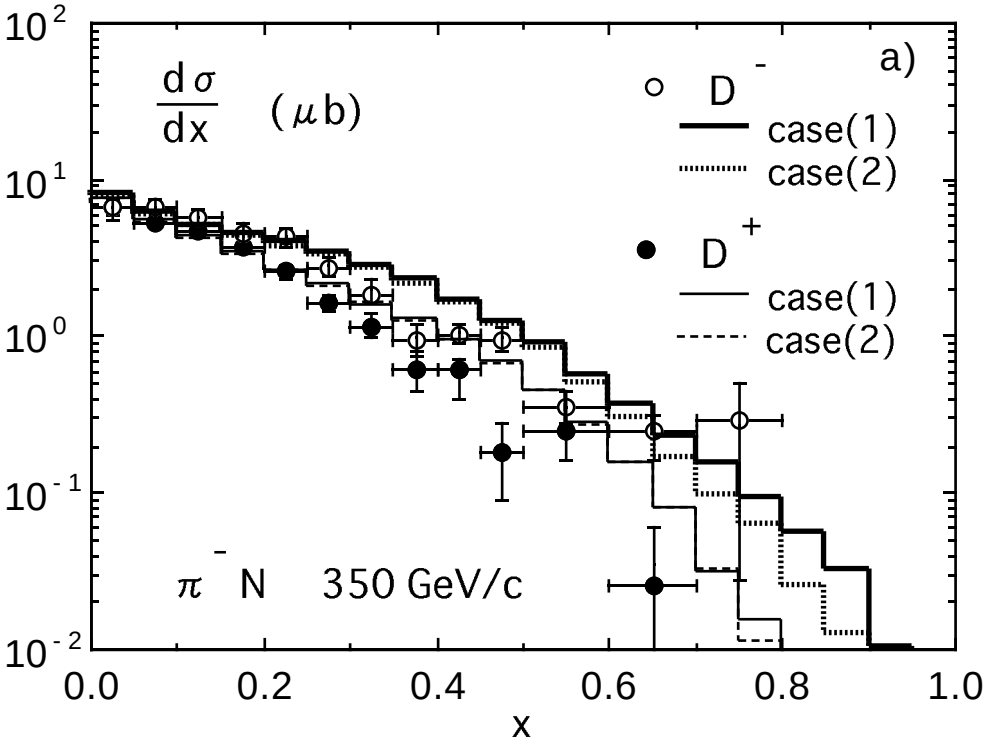
10^2
10^1
10^0
10^{-1}
10^{-2}
$\frac{d\sigma}{dx}$ (μb)
a)
D^-
case(1)
case(2)
D^+
case(1)
case(2)
π^- N 350 GeV/c
0.0
0.2
0.4
0.6
0.8
1.0
x

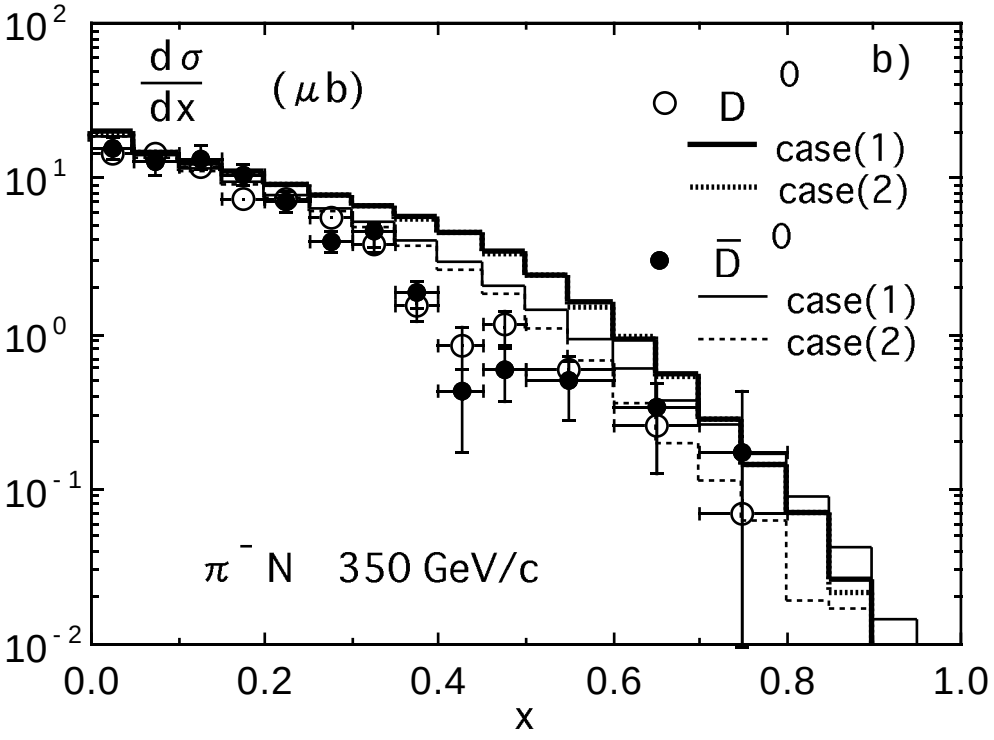
10^2
10^1
10^0
10^{-1}
10^{-2}
$\frac{d\sigma}{dx}$ (μb)
b)
D^0
case(1)
case(2)
$\bar{D}^0$
case(1)
case(2)
π^- N 350 GeV/c
0.0
0.2
0.4
0.6
0.8
1.0
x

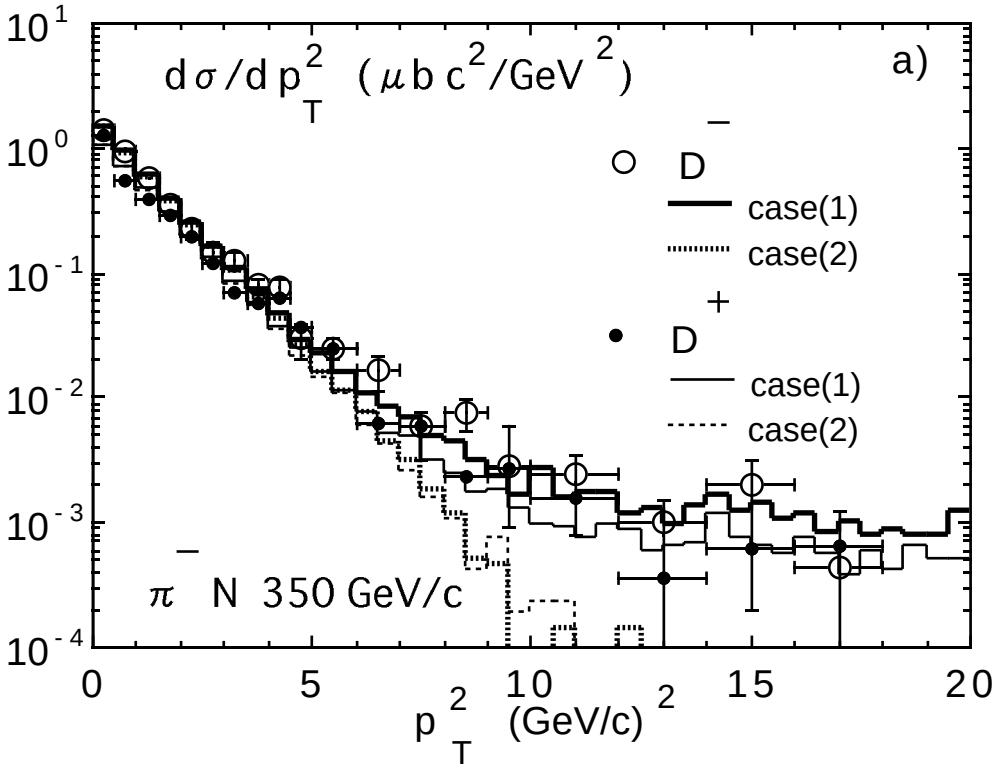
$d\sigma/dp_T^2$ ($\mu b\, c^2/GeV^2$)
a)
D^-
case(1)
case(2)
D^+
case(1)
case(2)
π^- N 350 GeV/c
10^1
10^0
10^{-1}
10^{-2}
10^{-3}
10^{-4}
0
5
10
15
20
p_T^2 $(GeV/c)^2$

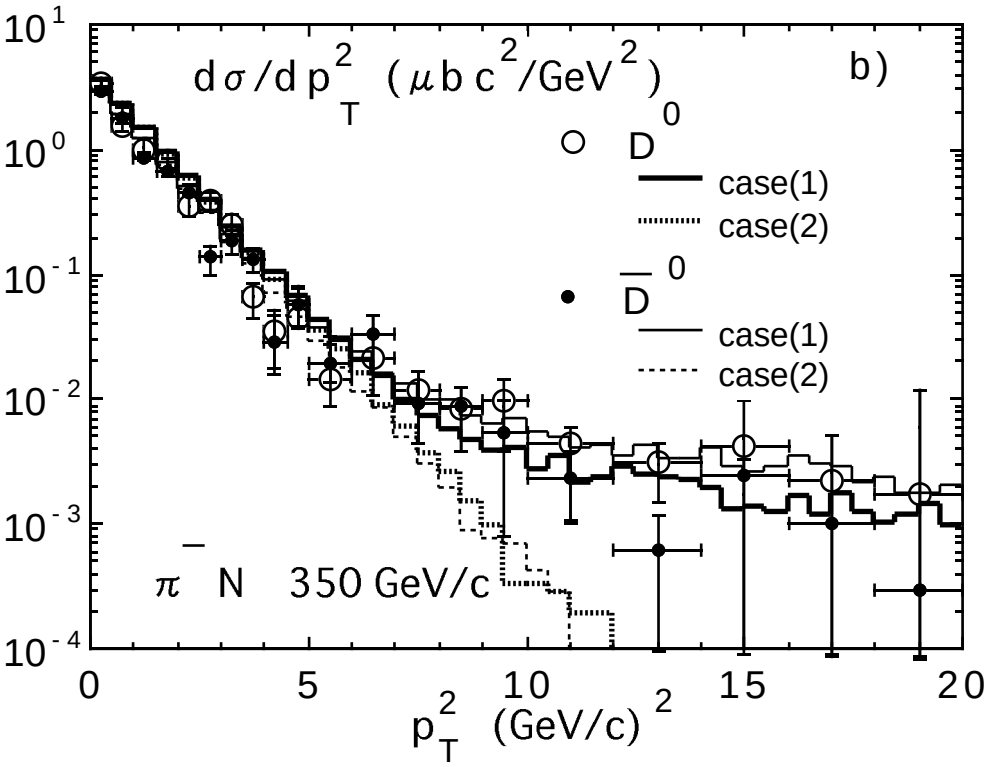
$d\sigma/dp_T^2$ ($\mu b\, c^2/GeV^2$)
b)
D^0
case(1)
case(2)
$\bar{D}^0$
case(1)
case(2)
π^- N 350 GeV/c
10^1
10^0
10^{-1}
10^{-2}
10^{-3}
10^{-4}
0
5
10
15
20
p_T^2 $(GeV/c)^2$

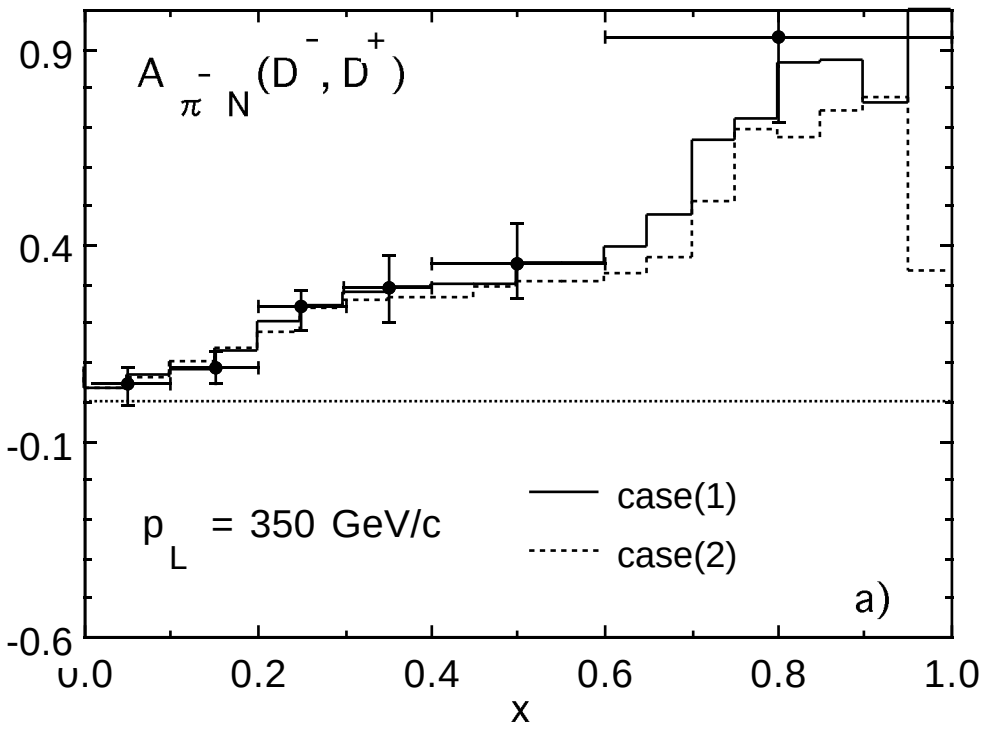
0.9
0.4
-0.1
-0.6
0.0
0.2
0.4
0.6
0.8
1.0
x
$A_{\pi^- N}(D^-, D^+)$
p_L = 350 GeV/c
case(1)
case(2)
a)

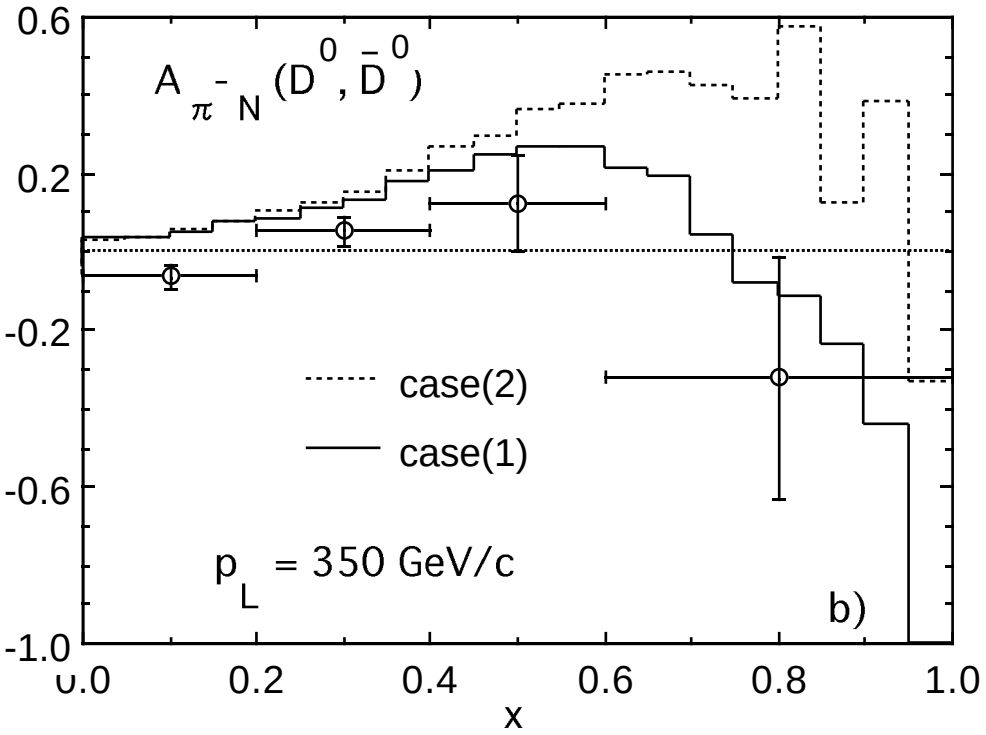
0.6
0.2
-0.2
-0.6
-1.0
0.0
0.2
0.4
0.6
0.8
1.0
x
$A_{\pi^- N}(D^0, \bar{D}^0)$
case(2)
case(1)
p_L = 350 GeV/c
b)

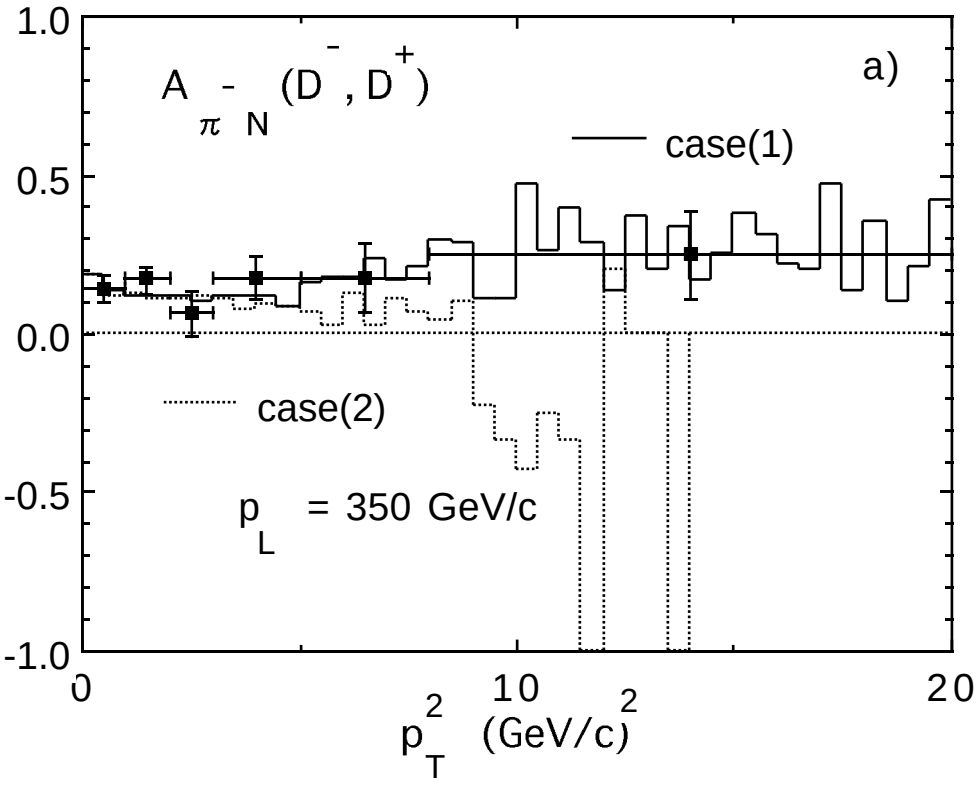
1.0
0.5
0.0
-0.5
-1.0
0
10
20
p_T^2 (GeV/c)^2
$A_{\pi N}(D^-, D^+)$
a)
case(1)
case(2)
p_L = 350 GeV/c

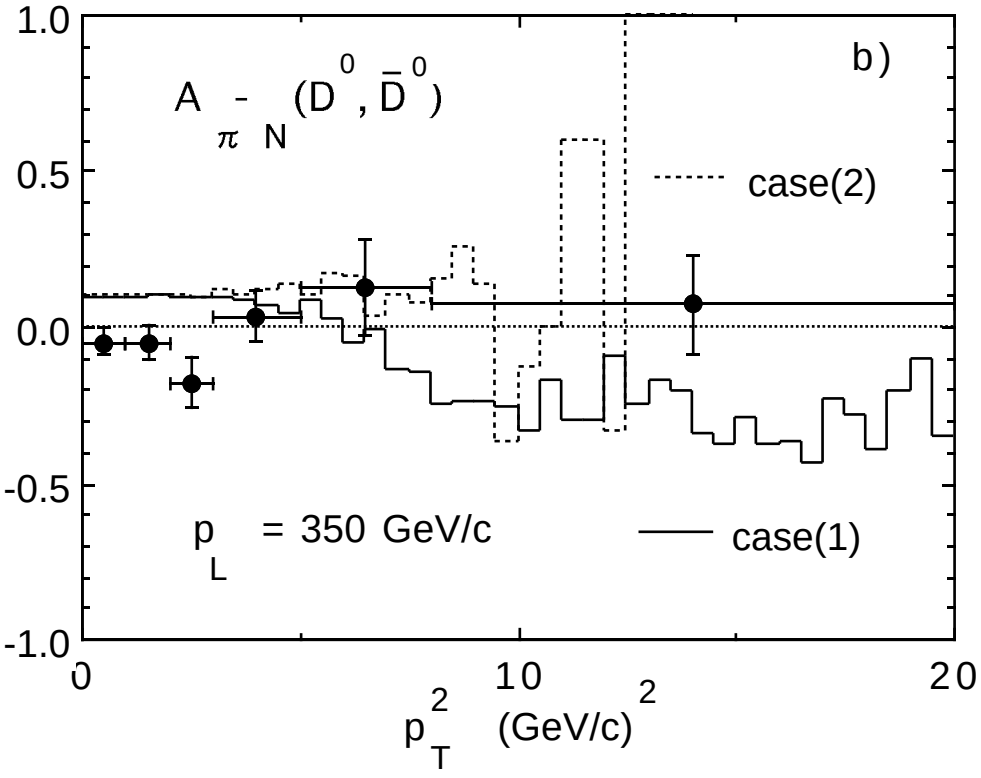
1.0
0.5
0.0
-0.5
-1.0
0
10
20
p_T^2 (GeV/c)^2
$A_{\pi N}(D^0, \bar{D}^0)$
b)
case(2)
case(1)
p_L = 350 GeV/c

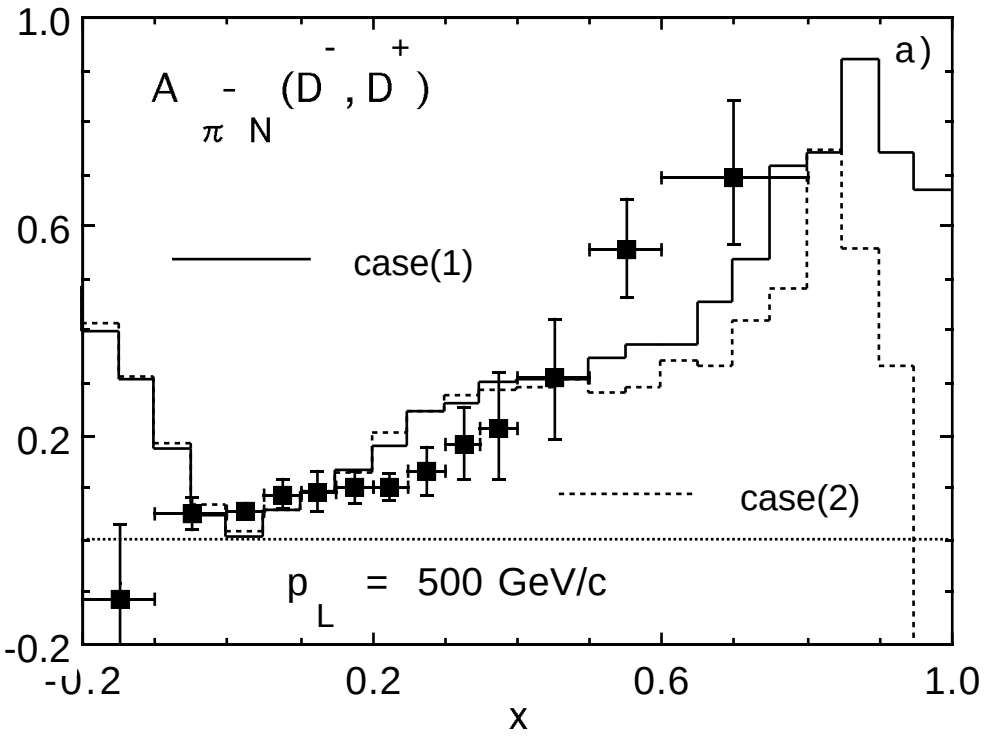
a)
A π - N (D-, D+)
case(1)
case(2)
p L = 500 GeV/c
1.0
0.6
0.2
-0.2
-0.2
0.2
0.6
1.0
x

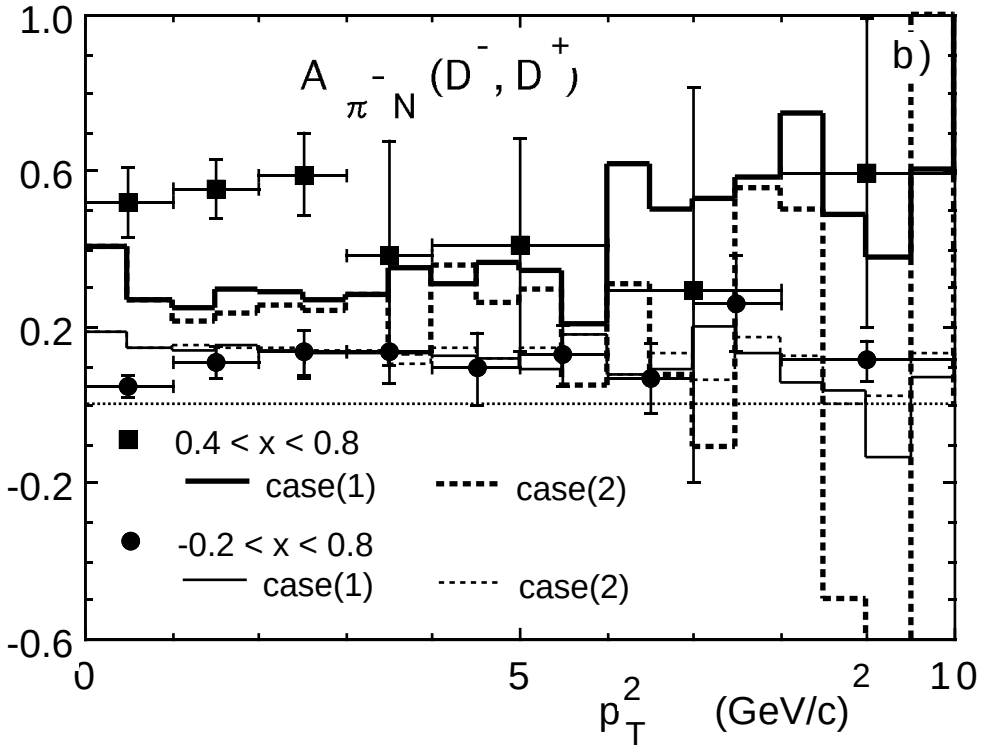
b)
A π - N (D-, D+)
0.4 < x < 0.8
case(1)
case(2)
-0.2 < x < 0.8
case(1)
case(2)
1.0
0.6
0.2
-0.2
-0.6
0
5
10
p2T (GeV/c)2

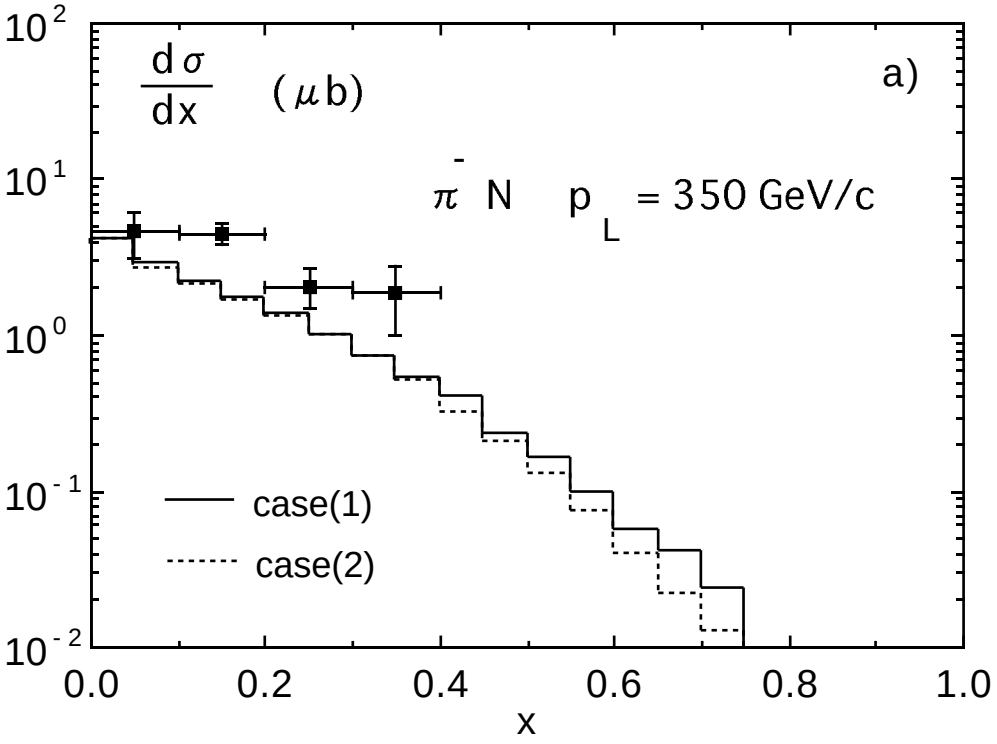
$\frac{d\sigma}{dx}$ (μb)
a)
π^- N p_L = 350 GeV/c
case(1)
case(2)
10^2
10^1
10^0
10^{-1}
10^{-2}
0.0
0.2
0.4
0.6
0.8
1.0
x

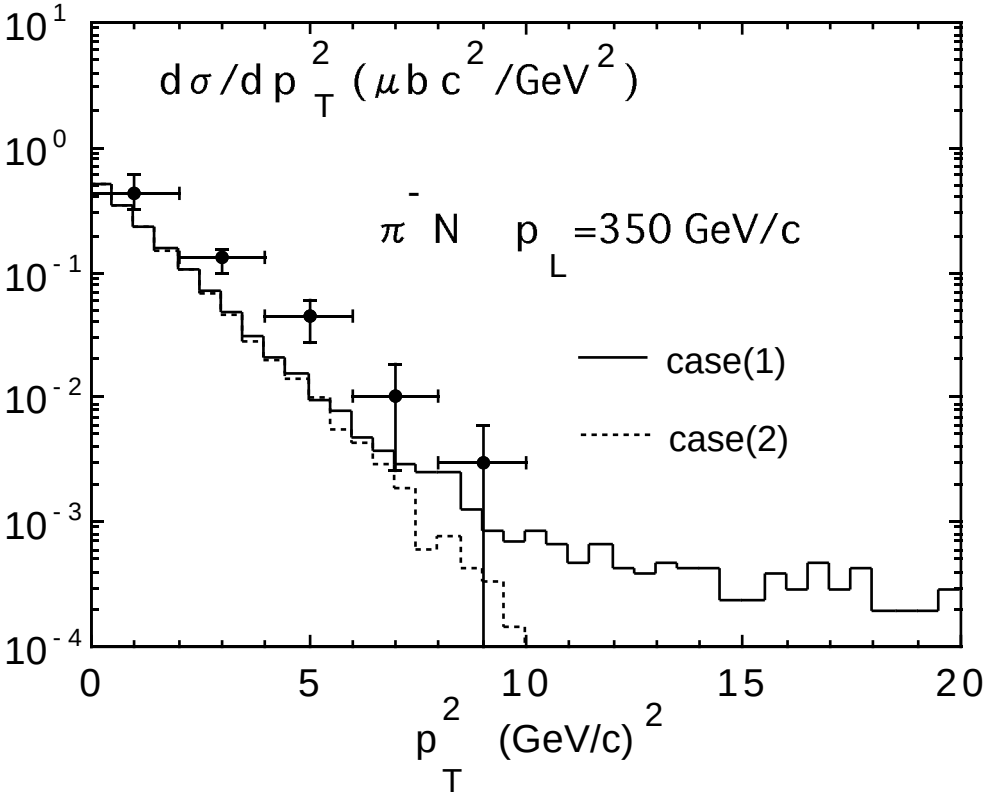
$d\sigma/dp_T^2$ (μb c^2/GeV^2)
π^- N p_L =350 GeV/c
case(1)
case(2)
10^1
10^0
10^{-1}
10^{-2}
10^{-3}
10^{-4}
0
5
10
15
20
p_T^2 (GeV/c)^2

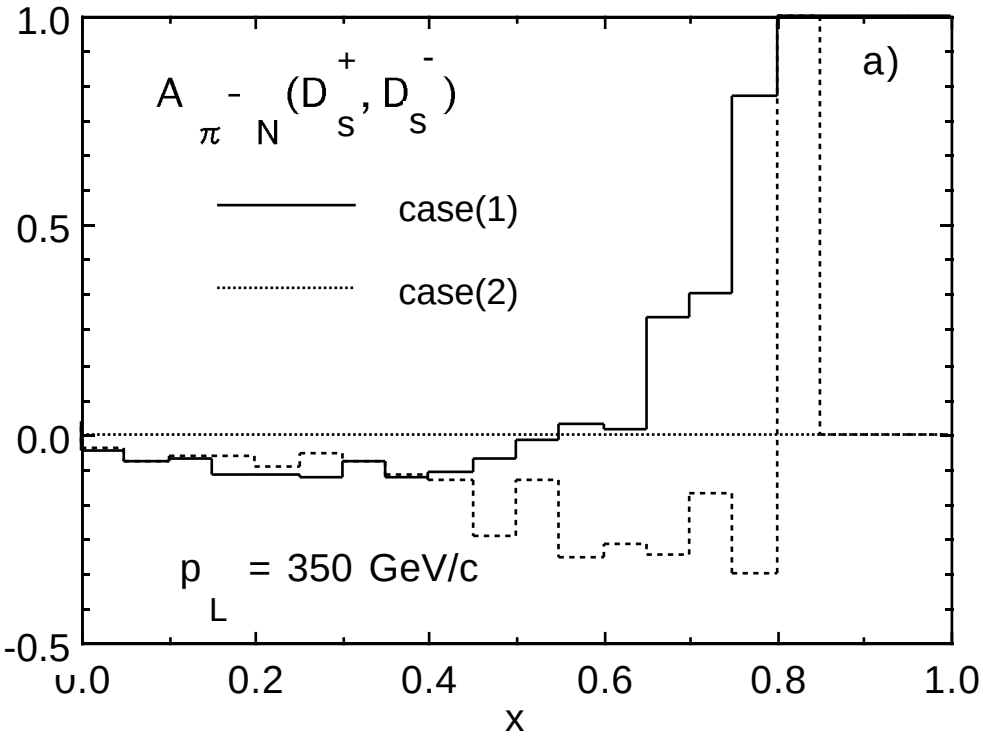
1.0
0.5
0.0
-0.5
0.0
0.2
0.4
0.6
0.8
1.0
x
a)
A π - N (D s+, D s-)
case(1)
case(2)
p L = 350 GeV/c

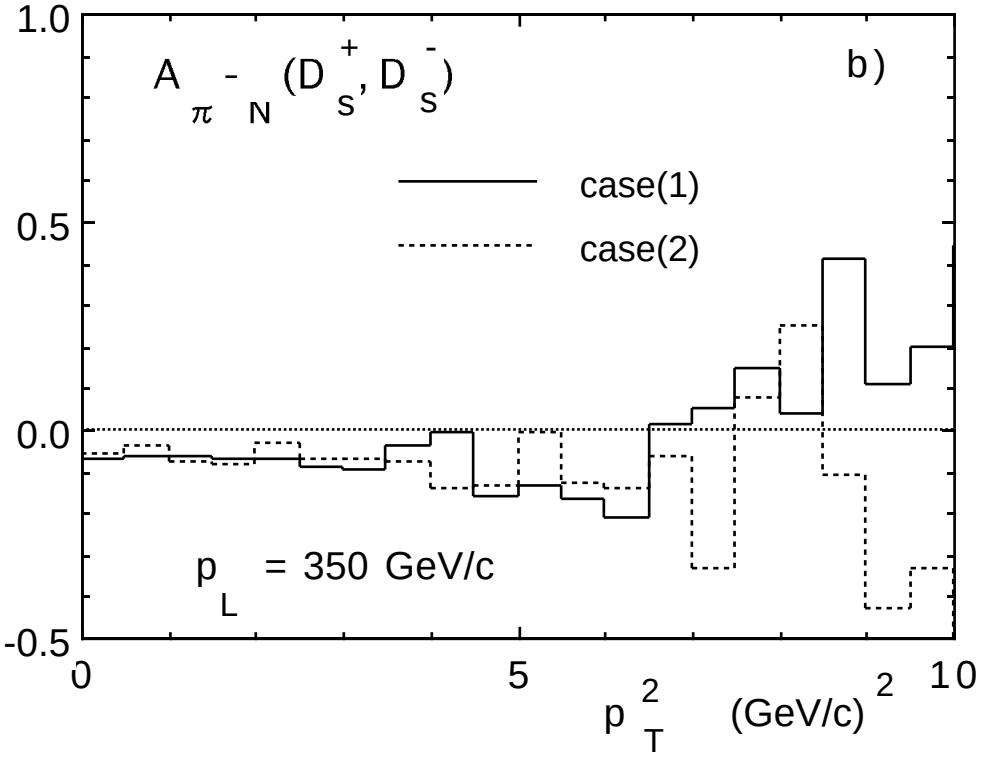
1.0
0.5
0.0
-0.5
0
5
10
p T 2 (GeV/c) 2
b)
A π - N (D s+, D s-)
case(1)
case(2)
p L = 350 GeV/c